PROBLEMY MECHATRONIKI
UZBROJENIE, LOTNICTWO, INŻYNIERIA BEZPIECZEŃSTWA

ISSN 2081-5891

12, 4 (46), 2021, 29-42

PROBLEMS OF MECHATRONICS
ARMAMENT, AVIATION, SAFETY ENGINEERING

A Method for Predicting Efficiency of Perforated Muzzle Brakes

Marta CZYŻEWSKA*, Radosław TRĘBIŃSKI

Military University of Technology, Faculty of Mechatronics, Armament and Aerospace
2 Sylwestra Kaliskiego Str., 00-908 Warsaw, Poland
**Corresponding author's e-mail address and ORCID*:
marta.czyzewska@wat.edu.pl; https://orcid.org/0000-0002-6382-335X

Received: July 12, 2021 / Revised: August 8, 2021 / Accepted: August 24, 2021 / Published: December 30, 2021

DOI 10.5604/01.3001.0015.5985

Abstract. This paper presents a method for predicting a value of a gasdynamic efficiency coefficient for perforated muzzle brakes. The method is based on the interior ballistics modelling for determining gasdynamic flow parameters at the brake inlet and 2D modelling the processes inside the brake with treating vents as circumferential slots. The modelling provides information about the mass flux time changes at the inlet and at the outlet of the brake. Using this information, the mass partition coefficient values and the gasdynamic efficiency coefficient values are calculated. It has been shown that the mass partition coefficient establishes very quickly and it is determined only by the geometry of the brake. The gasdynamic efficiency coefficient establishes after a relatively long time, what demands carrying out calculations for a relatively long time period. However, it has been shown that this problem can be solved by making use of the established ratio of mass fluxes at the outlet and the inlet.

So, flow parameters' values at the inlet are sufficient for determining the gasdynamic efficiency coefficient to the moment of attaining the final value. It has been shown that this value depends on the ballistics and on the vents inclination angle.
Keywords: ballistics, muzzle brake, gasdynamic efficiency coefficient

1. INTRODUCTION

In the process of design of muzzle brakes, it is desirable to assess their gasdynamic efficiency coefficient by using simulation tools. The coefficient is defined as ([1]):

$$\beta = \frac{I_{w0} - I_w}{I_{w0} - Mu_p} \tag{1}$$

where I_{w0}, I_w mean the recoil impulse without and with a brake, respectively, M is the projectile mass, and u_p is the muzzle velocity of the projectile. Values of all quantities in Eq. 1 can be calculated by the use of computational fluid dynamics methods. The values of I_{w0} and u_p can be calculated by using interior ballistics codes. But determining the I_w value is much more complicated, because gasdynamic processes, taking place in brakes, are quite complicated and they generally need 3D modelling. This problem was solved in [1] by applying 3D modelling to the flow through a single vent. It was taken into account that the flow inside the vent is established in a time scale much shorter than a time scale of the flow in the brake. Therefore, the flow can be treated as quasi-steady one. Moreover, the flow depends solely on the flow parameters in the main channel of the brake upstream of the vent. Basing on it, relations between the established flow parameters in a vent and flow parameters in the main channel were found. They were used for 1D modelling of the flow in the main channel. The outflow to the vents was taken into account by incorporating source terms in the 1D flow equations. Values of parameters at the brake inlet were calculated by an internal ballistic code.

For calculating the I_w pressure distribution on the vents, the side walls were used. So, the I_w value was calculated as:

$$I_w = A\int_0^\infty p_b dt - \sum_{n=1}^{N} \int_0^\infty \int_{S_n} p_n n_x dS_n \, dt \tag{2}$$

where A is the bore area, p_b is the breech pressure, p_n is the time- and position-dependent pressure acting upon the vent surface S_n, n_x is the axial component of the unit vector normal to the vent surface element dS_n, and N is the number of the vents. The model proposed in [1] was verified experimentally in [2] and [3].

Gasdynamic processes in perforated muzzle brakes were modelled in [4-6]. However, the problem of determining the gasdynamic efficiency coefficient was not addressed. In this work, a novel method for predicting this value is proposed.

It is much simpler than the method used in [1]. The method does not need information about the pressure distribution inside the vents (as in Eq. 2) and it bases solely on flow parameters' values at the brake inlet and the brake outlet. The objective of this work is to demonstrate the idea of the method, without aiming to attain high accuracy. That is why relatively simple models of the gasdynamic processes are applied.

2. METHODS

The gasdynamic flow behind the projectile, when it reaches the muzzle, is supersonic or close to sonic. In the first case, the flow at the muzzle remains supersonic for a time after the projectile leaves the muzzle. Then, it becomes subsonic. But the rarefaction wave entering the muzzle accelerates the flow. As a consequence, the flow at the muzzle becomes sonic. It also becomes sonic in the case, when initially the flow approaching the muzzle is subsonic. So, the flow at the muzzle is both supersonic or subsonic. A presence of a brake does not change this. It means, that the parameters' values of the flow at the brake inlet can be determined basing solely on the solution of the interior ballistics problem.

In this work, a relatively simple 1D single-phase model of the interior ballistics is used. Its simplicity is justified by the objective of this work. The model uses characteristic form of the flow equations:

$$dp \pm \rho c du = F\left(x, \rho, p, u, c, z\right) dt, \quad dx = \left(u \pm c\right) dt \tag{3}$$

$$F = F_1\left(\rho, p, c, z\right) - 2c^2 \rho u \frac{d \ln d(x)}{dx} \tag{4}$$

$$F_1 = \frac{\rho^2 c^2}{k} G\left(z\right) f_s\left(p\right)\left(\frac{f}{p} + \eta - \frac{1}{\rho_p}\right) - \frac{\rho^2 c^2 \left(k-1\right)}{kp\rho} f_h \tag{5}$$

$$\frac{d \ln \Phi}{dt} = H\left(\rho, p, c, z\right), \quad dx = u dt \tag{6}$$

$$H = \frac{\rho^2 c^2}{kp^2}\left\{\left[f + \left(k-1\right) p\left(\frac{1}{\rho_p} - \eta\right)\right] G\left(z\right) f_s\left(p\right) - \left(k-1\right)\frac{f_h}{\rho}\right\} \tag{7}$$

$$\Phi = p\left(\frac{1}{\rho} - \frac{1-z}{\rho_p} - \eta z\right)^k \tag{8}$$

where t is the time, x is the axial coordinate, $d(x)$ is the diameter of the bore, u is the flow velocity, p is the pressure, ρ is the density, c is the sound velocity, z is the relative burnt mass of the propellant, k is the specific heat ratio, η is the covolume in the Noble-Abel equation of state, f is the propellant force, and ρ_p is the propellant density.

The functions $G(z)$ and $f_s(p)$ are the functions in the burning law introduced in [7]:

$$\frac{dz}{dt} = G(z)\, f_s(p), \quad f_s(p) = p_0 \left(\frac{p}{p_0} \right)^n, \quad p_0 = 0{,}1\,\text{MPa} \tag{9}$$

The symbol f_h is the energy flux due to heat losses [8]:

$$f_h = 35.36 \frac{\rho u^{0.8}}{d} \left(\frac{D}{\rho d} \right)^{0.2} (T - 293); \quad D = \frac{378}{T+105} \left(\frac{T}{273} \right)^{1,5} \tag{10}$$

where T is the temperature.

The initial and boundary conditions are as follows:

$$\rho(x,0) = \Delta = \frac{m_p + m_{ign}}{V_0}, \quad u(x,0) = 0, \quad p(x,0) = p_f \tag{11}$$

$$z(x,0) = \frac{\Delta^{-1} - \rho_p^{-1}}{f p_f^{-1} - \rho_p^{-1} + \eta} \tag{12}$$

$$u(0,t) = 0, \quad u(x_p,t) = v_p(t) \tag{13}$$

where m_p is the propellant mass, m_{ign} is the igniter mass, V_0 is the initial volume inside the case, p_f is the forcing pressure value, v_p is the projectile velocity, and x_p is the distance the projectile travels:

$$\frac{dx_p}{dt} = v_p(t), \quad \frac{dv_p}{dt} = \frac{A_{in}}{m_{pre}} \left[p(x_p,t) - p_r(x_p, v_p) \right], \quad m_{pre} = m_{pr} \left(1 + \frac{\pi^2}{2T_w^2} \right) \tag{14}$$

where m_{pr} is the projectile mass, A_{in} is the surface area of the bore cross section (it is also the surface area of the brake inlet), and T_w is the pitch of rifling expressed in calibres. The resistance pressure p_r is a sum of the pressure of the air compressed by the projectile motion p_g and the resistance pressure p_{re} attributed to the projectile engraving process and the friction.

The boundary condition changes after the projectile has left the muzzle. When the flow is supersonic, the no reflective boundary condition is set. When the flow becomes subsonic, it is assumed that the flow is accelerated to the sonic flow by a rarefaction wave. The following relations are used for calculation of flow parameters' values at the muzzle:

$$p = p_a \left(\frac{u_a + b}{c_a + b} \right)^{\chi}, \quad \chi = \frac{2k}{k-1}, \quad b = \frac{\chi p_a}{\rho_a c_a} \tag{15}$$

$$u = c = c_a \left(\frac{p}{p_a} \right)^{1/\chi}, \quad \rho = \frac{kp}{c^2} \tag{16}$$

The subscript *a* denotes the parameters of the flow approaching the muzzle. The set of equations is solved by replacing differentials by finite differences and constructing solution of the finite difference equations on the characteristics net.

The flow in the muzzle brake is treated as 2D axially symmetric flow. The real set of vents is replaced by a set of circumferential slots with preservation of the venting area. Such an approach was used in [5] and the calculated blast characteristics were close to experimentally determined ones in [3]. The approach is based on the observed regularity that the gasdynamic efficiency is determined mainly by the ratio of the vent area to the area of the brake outflow and weakly depends on the shape of vents ([2]).

It is assumed that the propellant is completely burnt before the projectile leaves the muzzle. The propellant gases are treated as a perfect gas, because at relatively low pressure values the covolume can be disregarded. The flow in the brake is described by the set of equations:

$$\rho_{,t} + \left(\rho u_x\right)_{,x} + r^{-1}\left(r\rho u_r\right)_{,r} = 0 \tag{17}$$

$$\left(\rho u_x\right)_{,t} + \left(\rho u_x^2\right)_{,x} + r^{-1}\left(r\rho u_x u_r\right)_{,r} + p_{,x} = 0 \tag{18}$$

$$\left(\rho u_r\right)_{,t} + \left(\rho u_x u_r\right)_{,x} + r^{-1}\left(r\rho u_r^2\right)_{,r} + r^{-1}\left(rp\right)_{,r} = 0 \tag{19}$$

$$\left(\rho e\right)_{,t} + \left(\rho e u_x\right)_{,x} + r^{-1}\left(r\rho e u_r\right)_{,r} + \left(p u_x\right) + r^{-1}\left(r p u_r\right)_{,r} = 0 \tag{20}$$

$$e = \varepsilon + \tfrac{1}{2}\left(u_x^2 + u_r^2\right), \quad \varepsilon = \frac{p}{\rho(k-1)} \tag{21}$$

where u_x, u_r are the axial and radial velocity components, respectively, and ε is the specific internal energy.

The time period of projectile movement inside the brake is two order of magnitude shorter than the time in which the process inside the brake is modelled. So, we can neglect this period in modelling the processes in the brake. It is assumed that the process of venting starts when the projectile leaves the brake. So, initially the values of flow parameters are uniform across the brake and they are equal to the parameters at the brake inlet. It constitutes the initial conditions for solving the set of Eqs. (17-20).

The no permeable boundary condition was set at the brake inner walls. At the outlet of the brake and the outlets of vents, no reflective boundary condition was assumed. At the brake inlet, parameter values are determined by the solution of the interior ballistics problem.

The set of Eqs. (17-20) was solved by the use of the Fluent module of ANSYS 19.2.

Basing on the results of modelling, the mass fluxes at the inlet $q_{\min}$ and outlet q_{mou} of the brake are calculated. The coefficient of mass partition is calculated as the ratio of the mass passing the brake outlet and the mass entering the brake:

$$\alpha(t) = \frac{\int_{t_0}^{t} q_{mou}(t)dt}{\int_{t_0}^{t} q_{\min}(t)dt} \tag{22}$$

where t_0 is the moment of time when the projectile leaves the muzzle.

We assume that the impulse, produced by the brake {the second summand in Eq. (2)}, is equal to the change of the axial component of momentum of the gas that outflows from the vents. In the case of vents, perpendicular to the brake axis, this change of momentum is equal to the momentum of gas entering the brake. So, the impulse can be calculated as:

$$I_h(t) = \int_{t_0}^{t} \left[q_{\min}(t) - q_{mou}(t) \right] u_{in}(t)\, dt \tag{23}$$

The rarefaction wave, that enters the bore of the gun, moves upstream. So, it reaches the breech after a relatively long time. At this time, the pressure value at the breech becomes very low. So, the wave practically does not affect the value of the impulse exerted on the recoil parts of the gun. It means that the numerator in Eq. (1) reduces to I_{h}. On the other hand, the impulse value, exerted on the recoil parts to the moment the projectile leaves the muzzle, is close to the momentum value of the projectile. So, the denominator in Eq. (1) can be approximated by:

$$I_{w1}(t) = A_{in} \int_{t_0}^{t} p_b dt \tag{24}$$

The value of the gasdynamic efficiency coefficient is therefore approximated by the formula:

$$\beta(t) = \frac{I_h(t)}{I_{w1}(t)} \tag{25}$$

The coefficients α and β are represented as functions of time, because simulations of the processes in the brake can be made only in a finite time.

Analysing asymptotic behaviour of these functions, we can infer concerning their values in infinity.

The approach, described above, can be applied for determining the value of β for the brakes with vents perpendicular to the brake axis. In the case of brakes with vents, inclined to the brake axis, Eq. (23) should be replaced by:

$$I_h(t) = \int_{t_0}^{t} \left[q_{\min}(t) - q_{mou}(t) \right] \left[u_{in}(t) - u_v(t) \cos\varphi \right] dt \tag{26}$$

where u_v is the effective velocity of the flow through the vents, φ is the angle between the axis of vents and the brake axis (< 90° for vents inclined towards the brake outlet, > 90° for vents inclined towards the brake inlet). A rough estimation of u_v value is considered:

$$u_v(t) = u_{in}(t) \tag{27}$$

This approximation gives an upper limit of the u_v value.

3. RESULTS AND DISCUSSION

The interior ballistics problem was solved for a 35 mm antiaircraft gun, for two types of ammunition FAPDS-T and TP-T. The calculated muzzle velocity values are 1474 and 1202 m/s, respectively (1440 and 1180 m/s are catalogue values). Figures 1 and 2 present the results of calculations of pressure, velocity, and density values at the muzzle brake inlet in the form of plots of relative changes of these values in time.

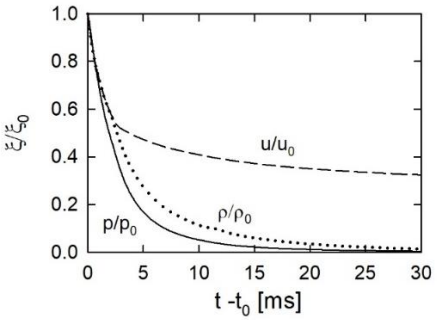

Fig. 1. Plots of relative time changes of pressure, velocity, and density values, FAPDS-T

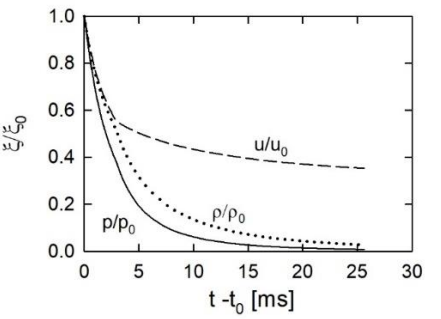

Fig. 2. Plots of relative time changes of pressure, velocity, and density values, TP-T

Pressure and density values decrease relatively quickly, whereas velocity values decrease relatively slowly from the moment when the rarefaction wave enters the muzzle. It is a result of acceleration of the flow by the rarefaction wave.

For 2D simulations of the processes in the brake, plots shown in Figs. 1 and 2 were approximated by the function:

$$\xi = \frac{\xi_{0i}}{1 + a_{1i}\left(t - t_{0i}\right) + a_{2i}\left(t - t_{0i}\right)^2} \tag{28}$$

the quantities $\xi_{0i} = \{p_{0i}, u_{0i}, \rho_{0i}\}$ are the values of the pressure, velocity, and density at the time moment t_{0i} (t_{01} corresponds to the moment when projectile leaves the muzzle, t_0, t_{02} to the moment when the flow at the brake inlet becomes sonic).

Figure 3 presents time changes of the impulse I_{w1} exerted on the breech of the gun after the projectile has left the muzzle. The impulse reaches its limiting value: 274 Ns for FAPDS-T and 218 Ns for TP-T shortly after the rarefaction wave reaches the breech.

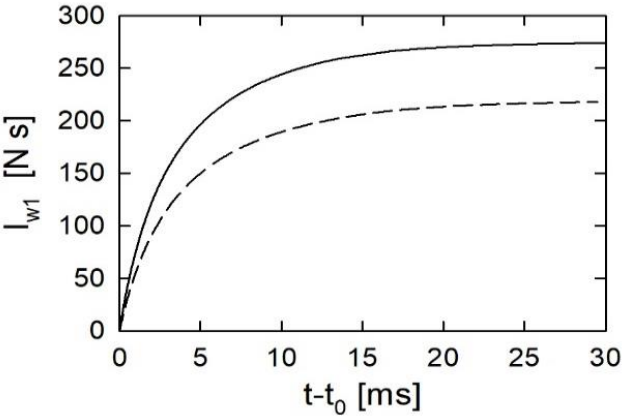

Fig. 3. Evolution in time of the impulse I_{w1}: solid line FAPDS-T, dashed line TP-T

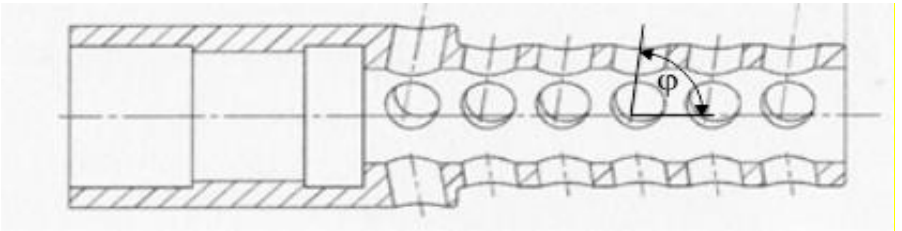

Fig. 4. Sketch of the cross section of the modelled muzzle brake (φ= 82°)

Geometry of an existing muzzle brake, shown in Fig. 4, was chosen to be a basis for 2D simulations. Each set of vents was replaced by a circumferential slot with preserving the venting area. The centre plane of the slot coincides with the axis of vents. In order to analyse influence of the vent axis inclination angle φ on β values, three variants were considered: $\varphi = 90^o$, 82^o, and 98^o.

Figure 5 presents the velocity values distribution at a moment of time. It illustrates well the wave picture of the processes inside the brake. At the windward edges of vents, Prandtl-Meyer flow is generated. It causes a turning of the flow. Then, it turns again in the shock wave that is generated at the leeward edge of the vent. The shock wave reflects at the axis of the brake and the Mach stem is generated. The reflected waves interfere with the shock waves originating from the consecutive vent edges.

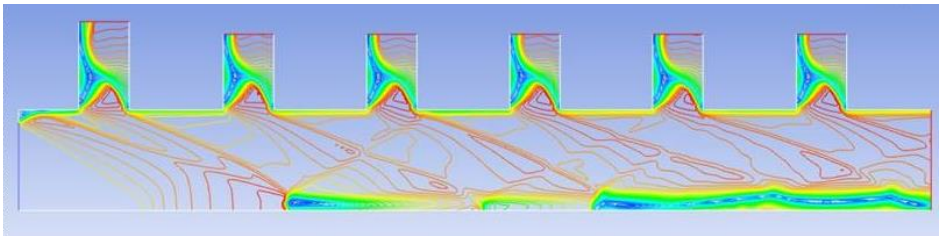

Fig. 5. Exemplary velocity values distribution in the brake

Figure 6 presents plots of the mass partition coefficient. After a transient time, the value of the coefficient establishes. This value does not depend on the type of ammunition. It means that it solely determined by the geometry of a brake. So, it can be considered as a characteristics of a brake.

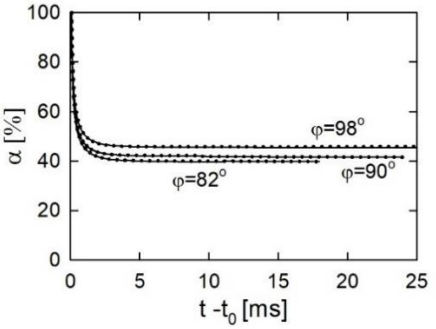

Fig. 6. Plots of the mass partition coefficient; solid line FAPDS-T, dotted line TP-T

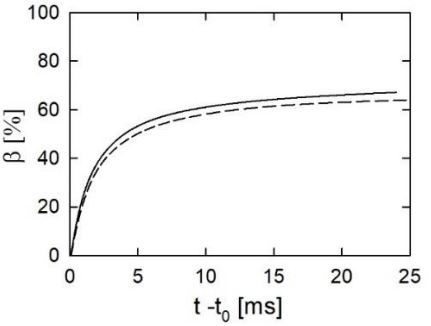

Fig. 7. Plots of the gasdynamic efficiency coefficient ($\varphi = 90^o$); solid line FAPDS-T, dashed line TP-T

The values of gasdynamic efficiency coefficient show a dependence on the type of ammunition (Fig. 7). It is in agreement with experimental observations (see reference [2]) that β value mildly depends on ballistics.

The influence of the vents inclination angle is illustrated by the plots shown in Figs. 8 and 9. The obtained results are qualitatively correct. Diminishing the inclination angle value leads to the lower turning angle of the flow. The turning angle in the Prandtl-Meyer flow does not change, but the turning angle in the shock wave decreases. It means that the shock wave is less intensive. So, the difference of pressure values on the vent opposite walls is lower and hence, the I_h value is lower. It causes diminishing the β value. Just opposite situation takes place when the inclination angle value is higher than 90°. The turning angle value of the flow is higher and the shock wave is more intense. As a consequence, the value of β should be higher than that for the vents perpendicular to the brake axis.

The experimental data, concerning the effect of the inclination angle, are scarce. In [2], for perpendicular vents β = 51.1%, while for the vents inclined by 100° β = 55.1%. This result in qualitative agreement with the results shown in Figs. 8 and 9. The difference between these values of β (4%) is of the same order of magnitude as the difference predicted in this work (FAPDS-T: 6.4% for φ = 82°, 5.1% for φ = 98°, TP-T: 7% for φ = 82°, 4.6% for φ = 98°). However, taking into account that Eq. (27) predicts the upper limit of the u_v value, we can expect that the effect of the inclination angle value is weaker than the predicted one.

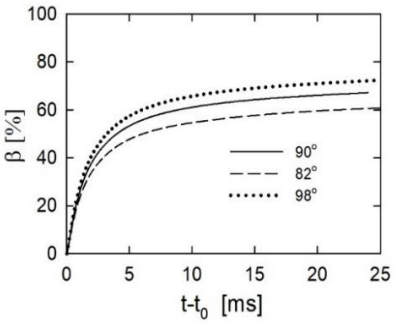

Fig. 8. Plots of the gasdynamic efficiency coefficient for various values of the inclination angle, FAPDS-T

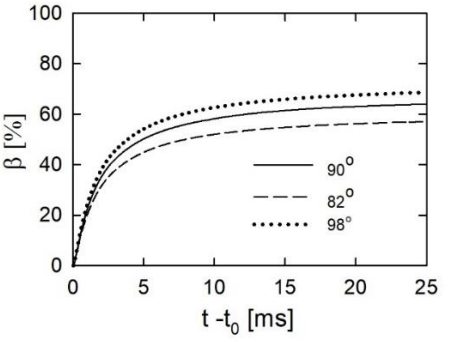

Fig. 9. Plots of the geodynamic efficiency coefficient for various values of the inclination angle, TP-T

Whereas the mass partition coefficient quickly attains its final value, the gasdynamic efficiency coefficient continuously increases.

It is caused by relatively slow diminishing the velocity value at the brake inlet and relatively quick establishing the I_{w1} value. This behaviour of the function $\beta(t)$ demands relatively long time of calculations. It is computationally expensive, especially when 3D modelling is performed. But, we can solve this problem by making use of the observed establishing the α value. It suggests that the ratio of the fluxes $q_{\text{mou}}/q_{\min}$ tends to a constant value. An exemplary plot, shown in Fig. 10, proves that the value of this ratio is not constant but it oscillates around the average value α^*. Because the amplitude of these oscillations is low, we can assume that after establishing the value α, the ratio $q_{\text{mou}}/q_{\min}$ is equal to α^*. The value α^* is somewhat lower than the value α (0.4 versus 0.42) what is an effect of the transient period. Using the value α^*, we can modify Eq. (26):

$$I_h(t) = I_h(t_1) + (1-\alpha^*)\int_{t_1}^{t} q_{\min}(t)\left[u_{in}(t) - u_v(t)\cos\varphi\right]dt \qquad (29)$$

The plots, shown in Fig. 11, enable us to make an assessment of accuracy of the above approximation. The results of calculations by Eq. (26) are compared with the results of calculations by Eq. (29) with t_1 = 10 ms. The comparison justifies the use of Eq. (29). This result is important, because it proves that the simulation of gasdynamic processes in the brake can be make for a restricted time period. For determining β values after this period only the values of parameters at the brake inlet are sufficient ones. This needs only the solution of the interior ballistics problem and it is much less computationally expensive than modelling processes inside the brake.

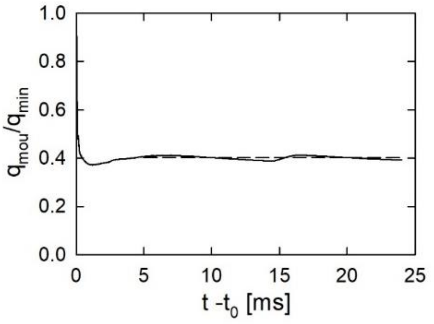

Fig. 10. Plot of q_{mou}/q_{min}; dashed line – average value; φ = 90°

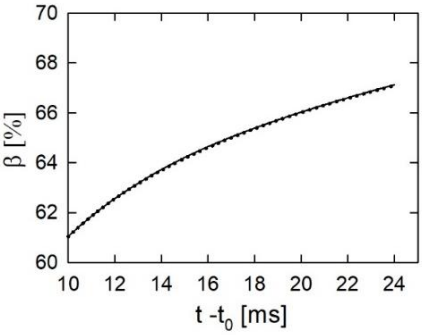

Fig. 11. Comparison of $\beta(t)$ plots: solid line - Eq.26, dotted line - Eq. 29

The plot $\beta(t)$ for FAPDS-T ammunition and φ = 90° is presented in Fig. 12 as an illustration of the results obtained by the use of Eq. (29). A value of β reaches its final value 70.2% after a relatively long time of 70 ms. This value can be compared with the value 77.5% calculated by the empirical formula proposed in [2]:

$$\beta = 0.273A_R\left[1-0.18L/D\right]\left(1-0.14A_R+0.01A_R^2\right) \tag{30}$$

where A_R is the ratio of the venting area to the area of the brake outlet (6 in the considered case), L/D is the ratio of the length and the diameter of vents (0.5 in the considered case). Taking into account approximate character of the model used in this work and approximate character of Eq. (30), the difference between these two values can be assessed as relatively low one.

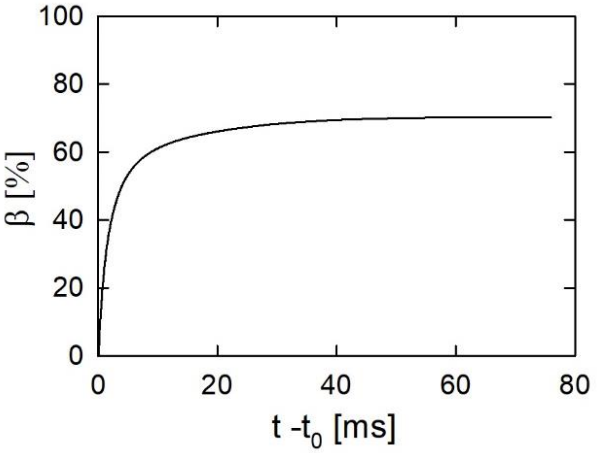

Fig. 12. $\beta(t)$ plot calculated by using Eq. 29, FAPDST-T, $\varphi = 90^o$

The value $\beta(t)$ changes quickly in the period of the transient process. The results of modelling in this period depend on formulation of the initial condition. The simplified initial condition, used in this work, lowers the β value. So, for increase in accuracy of determining this value, it is recommended to take into account the period in which the projectile moves through the brake.

4. CONCLUSIONS

The results of the presented analysis enabled us to recognise some problems connected with estimation of a value of the gasdynamic efficiency coefficient for perforated muzzle brakes on the basis of computational simulations of fluid dynamics. The main findings are as follows:

1. The mass partition coefficient value establishes at a relatively short time.
2. The mass partition coefficient value depends on the geometry of the brake and it does not depend on the ballistics parameters.
3. The gasdynamic efficiency coefficient reaches its final value after a relatively long time, what complicates estimating its value on the basis of simulations' results. However, this problem can be solved basing on the fact that the ratio of mass fluxes at the inlet and outlet establishes after a transient time.

The solution of the interior ballistics problem is sufficient to assess the value of β for a longer time.

4. The gasdynamic efficiency coefficient depends mildly on ballistics.
5. The proposed method of determining the gasdynamic efficiency coefficient gives rational results. However, the predicted influence of the vents inclination angle's value may be too strong.
6. The method can be easily adopted to more complicated 3D models of the processes in perforated muzzle brakes.

In the follow-up research, the authors intend to extend the presented analysis by making a comparison between 2D and 3D modelling results, taking into account the projectile motion through the brake, improving the estimation of u_v value and by experimental verification of the proposed method.

FUNDING

This work was supported by the Polish National Research Centre [grant number DOBR/0046/R/ID1/2012/03].

REFERENCES

[1] Carofano, G.C. 1988. *The Gasdynamics of Perforated Muzzle Brakes*. Technical Report ARCCBTR-88006, Benet Laboratories, Watervliet, NY.

[2] Carofano, G.C. 1993. *Perforated Brake Efficiency Measurements Using a 20-mm Cannon*. Technical Report ARCCB-TR-93010, US Army Armament Research, Development and Engineering Center, Close Combat Armaments Center, Benet Laboratories, Watervliet, N.Y.

[3] Carofano, G.C. 1990. *Comparison of Experimental and Numerical Blast Data for Perforated Muzzle Brakes*. Technical Report ARCCB-TR-90034, US Army Armament Research Development and Engineering Center, Close Combat Armaments Center, Benet Laboratories, Watervliet, N.Y.

[4] Guo, Zhangxia, Yutian Pan, Haiyan Zhang, and Baoquan Guo. 2013. "Numerical Simulation of Muzzle Blast Overpressure in Antiaircraft Gun Muzzle Brake". *Journal of Information & Computational Science* 10 (10) : 3013–3019.

[5] Semenov, Ilya, Pavel Utkin, Ildar Akhmedyanov, Igor Menshov, and Pavel Pasynkov. 2013. Numerical investigation of near-muzzle blast levels for perforated muzzle brake using high performance computing. In *International Conference "Parallel and Distributed Computing Systems" PDCS 2013*. Ukraine, Kharkiv, March 13-14, 2013.

[6] Chaturvedi, Ekansh, and Ravi Kumar Dwivedi. 2019. “Computer aided design and analysis of a tunable muzzle brake”. *Defence Technology* 15 : 89-94.

[7] Trębiński, Radosław, Zbigniew Leciejewski, Zbigniew Surma, and Bartosz Fikus. 2016. Some Considerations on the Methods of Analysis of Closed Vessel Test Data. In *Proceeding of the 29th International Symposium on Ballistics*, 9-13 May, 2016, Edinburgh, Great Britain, Vol. 1: pp. 607-617.

[8] Łazowski, Jerzy, Jerzy Małachowski, and Robert Kaminski. 2008. “MES Analysis of Heat Loading of Barrel during Shot” (in Polish). *Biuletyn WAT* 57 (1) : 215-228.

Metoda przewidywania skuteczności perforowanych hamulców wylotowych

Marta CZYŻEWSKA, Radosław TRĘBIŃSKI

Wojskowa Akademia Techniczna,
Wydział Mechatroniki, Uzbrojenia i Lotnictwa, Instytut Techniki Uzbrojenia
ul. gen. Sylwestra kaliskiego 2, 00-908 Warszawa

Streszczenie. W pracy przedstawiono metodę przewidywania wartości impulsowego współczynnika efektywności gazu dla perforowanych hamulców wylotowych. Metoda wykorzystuje modelowanie balistyki wewnętrznej do wyznaczania parametrów dynamicznego przepływu gazu na wlocie hamulca oraz dwuwymiarowy model procesów zachodzących wewnątrz hamulca, traktując boczne kanały wylotowe jako obwodowe otwory. Model ten dostarcza informacji o zmianach w czasie strumienia masy na wlocie i wylocie hamulca. Na podstawie tych informacji obliczane są wartości współczynnika podziału masy oraz impulsowego współczynnika efektywności gazu. Pokazano, że wartość współczynnika podziału masy ustala się bardzo szybko i jest determinowana jedynie geometrią hamulca. Wartość impulsowego współczynnika efektywności gazu ustala się po stosunkowo długim czasie, co wymaga przeprowadzenia obliczeń w relatywnie długim okresie. Pokazano jednak, że problem ten można rozwiązać, wykorzystując ustalony stosunek strumieni masowych na wylocie i wlocie hamulca.
Zatem wartości parametrów przepływowych na wlocie są wystarczające do wyznaczenia impulsowego współczynnika efektywności gazu w momencie osiągnięcia jego wartości końcowej. Wykazano, że wartość ta zależy od parametrów balistycznych i kąta nachylenia bocznych otworów wylotowych.
Słowa kluczowe: balistyka, hamulec wylotowy, impulsowy współczynnik efektywności hamulca